

7-28-2021

Experimental investigation on dynamic properties of soft clay under coupled cyclic-seepage loads

Hua-yang LEI

Key Laboratory of Earthquake Engineering Simulation and Seismic Resilience, China Earthquake Administration Tianjin 300350, China

Ying-gang XU

Department of Civil Engineering, Tianjin University, Tianjin 300350, China

Jiang-yan MIAO

Department of Civil Engineering, Tianjin University, Tianjin 300350, China

Xu LIU

Department of Civil Engineering, Tianjin University, Tianjin 300350, China

Follow this and additional works at: <https://rocksoilmech.researchcommons.org/journal>



Part of the [Geotechnical Engineering Commons](#)

Custom Citation

LEI Hua-yang, XU Ying-gang, MIAO Jiang-yan, LIU Xu, . Experimental investigation on dynamic properties of soft clay under coupled cyclic-seepage loads[J]. Rock and Soil Mechanics, 2021, 42(3): 601-610.

This Article is brought to you for free and open access by Rock and Soil Mechanics. It has been accepted for inclusion in Rock and Soil Mechanics by an authorized editor of Rock and Soil Mechanics.

Experimental investigation on dynamic properties of soft clay under coupled cyclic-seepage loads

LEI Hua-yang^{1, 2, 3}, XU Ying-gang¹, MIAO Jiang-yan¹, LIU Xu¹

1. Department of Civil Engineering, Tianjin University, Tianjin 300350, China

2. Key Laboratory of Coast Civil Structure Safety of Education Ministry, Tianjin University, Tianjin 300350, China

3. Key Laboratory of Earthquake Engineering Simulation and Seismic Resilience, China Earthquake Administration Tianjin 300350, China

Abstract: In this paper, a series of triaxial tests under coupled cyclic-seepage loads were carried out for saturated soft clay in Tianjin. The results show that the development of cumulative plastic strain is characterized by three stages: initial instantaneous growth, decelerated increase and stable / linear development, and seepage can enlarge the dynamic deformation up to 1–2 times of that compared to cyclic load only. Larger seepage force induces greater cumulative plastic deformation. The lower frequency or greater cyclic stress amplitude induces larger strain. The prediction model of cumulative plastic deformation of soft clay is established under the condition of dynamic-seepage coupling. The presence of seepage induces greater inclination to strain axis of hysteric curve at initial vibration. The dynamic elastic modulus of soft clay increases first and then decreases, and the larger seepage force induces lower modulus; the mathematical relationship between dynamic elastic modulus and cumulative plastic strain is revealed: under seepage condition, a prediction model of dynamic modulus was proposed considering the influences of seepage force and frequency. The damp ratio decreases to a constant value with increasing number of cycle. The larger the seepage force is, the larger the damping ratio attenuation amplitude is, and the damping ratio is approximately 0.02–0.04 at the end of the vibration. The results could provide guidance on the numerical simulation of dynamic characteristics of soft clay ground under seepage condition.

Keywords: soft clay; dynamic-seepage coupling; cumulative plastic strain; seepage; dynamic modulus; damping ratio

1 Introduction

With the development of national economy, the development of underground space has become an effective means to solve the problem of limited land resources that restricts urban development. Underground engineering (foundation pit engineering, tunnel engineering, underground utility tunnel, etc.) shows much deeper, larger, and longer characteristics adapted to sustainable development of cities^[1]. There are often two types of engineering risks in construction: high geological risks and high environmental risks. In coastal areas, the groundwater level is high, and there are soft soil layers, flowable silt layers and sand layers, which pose high geological risks. In addition, underground engineering is concealed, and it is difficult to repair construction defects and monitor service performance. There are dense surrounding overground and underground facilities, which makes the construction difficult. Moreover, it is important to ensure the safety of the existing underground structures in the vicinity, which poses high environmental risks. Effective and feasible development of underground space is of great significance to ensure safety of project construction and environment.

As the scale of engineering construction continues to increase, accidents frequently occur, such as excessive

ground settlement caused by underground excavation or major water inrush and sand inrush engineering accidents: tunnel excavation induced damage (such as flooding and collapse accident of the Foshan subway in 2018, the flooding and collapse accident of the Guangzhou Metro Line 1 in 2019, etc.); the engineering losses caused by the collapse of the foundation pit and the destruction of the surrounding environment (such as a collapse accident of the deep foundation pit in Nanjing due to water hazard in 2019, inclined cracking of surrounding buildings caused by water leakage of foundation pit of Tianjin Metro Line 3 in 2009, etc.). The causes of these underground engineering accidents are mostly related to groundwater. The potential threats of groundwater hazards to engineering construction and engineering service must be highly valued and deeply analyzed by researchers.

At present, for the dynamic loading analysis of soft clay, researchers have analyzed many influencing factors, including cyclic stress ratio^[2], vibration waveform^[3], vibration frequency^[4], consolidation state^[5–6], confining pressure^[7], and stress path^[8], etc. In general, these factors can be divided into two levels: the initial state of the soil and the load pattern. Regarding the dynamic deformation of soft clay, the main conclusions is that the development of deformation has three stages^[2, 9] with a critical cyclic stress ratio^[2, 7]. There is a controversy

Received: 28 June 2020

Revised: 24 December 2020

This work was supported by the National Key R&D Plan (2017YFC0805407), the Major Projects of the National Natural Science Foundation (51890911) and the Open Project Fund of State Key Laboratory of Disaster Reduction in Civil Engineering (SLDRCE17-01).

First: LEI Hua-yang, female, born in 1974, PhD, Professor, PhD supervisor, mainly engaged in geotechnical engineering teaching and scientific research.

E-mail: leihuayang74@163.com

about the influence of vibration frequency on deformation. Zheng et al.^[4] believed that frequency had little influence on deformation, while Lei et al.^[10] deemed that frequency had a great influence on deformation development, and developed a deformation development prediction model considering various factors by using empirical analysis. As for the engineering characteristics of soft clay in seepage field, many scholars mainly analyzed the permeability coefficient of soft clay from the perspective of unit tests, considering different loading modes^[11], characteristics of structure^[12], soil sample gradation^[13] and other aspects, and established different calculation models of permeability coefficient of soft clay, which provided a basis for the conversion of the permeability coefficient of soft clay under the certain initial conditions.

Soft clay often undergoes multi-field coupling in complex environments, such as unloading disturbances in foundation pit engineering, additional traffic loads from adjacent municipal road operations, and seepage effects caused by foundation pit dewatering, and combined cyclic loading of traffic and groundwater seepage during the operation period of the subway tunnel. Coupled effect of dynamic stress field and seepage field is more common in underground engineering problems. Therefore, accurate evaluation of the engineering characteristics for soft clay is of great significance for the design, construction, and operation safety analysis of underground engineering.

There are relatively few studies on the engineering response of soft clay under dynamic–seepage conditions, and thus further study is needed. This paper presents experiments on dynamic characteristics of soft clay under dynamic–seepage coupling conditions through the indoor cyclic triaxial test using the seepage module for the test instrument. The influences of seepage force on the hysteresis curve characteristics and damping ratio of soft clay are mainly analyzed; the development laws of the cumulative plastic strain for the soil under different seepage forces, frequencies and dynamic stress amplitudes are also analyzed. A model for prediction of the cumulative plastic deformation of soft clay in the dynamic–seepage field is developed. Meanwhile, the influencing factors of the dynamic elastic modulus of soft clay are analyzed, and the normalized conversion model of the dynamic elastic modulus is established to provide a basis for numerical analysis and theoretical research.

2 Test sample and scheme

2.1 Test sample

The test soil samples were taken from Tianjin Binhai New Area, with a depth of 10 m. A thin-walled soil sampler was used for sampling. Laboratory physical parameter test of soil was carried out, and the main physical and mechanical properties are shown in Table 1.

Table 1 Basic physical and mechanical properties of samples

Moisture content ω /%	Density ρ /($\text{g} \cdot \text{cm}^{-3}$)	Specific gravity G_s	Void ratio e_0	Liquid limit ω_L /%	Plastic limit ω_P /%	Permeability coefficient k_v /($\text{cm} \cdot \text{s}^{-1}$)	Cohesion c /kPa	Internal friction angle φ /($^\circ$)	Compression index C_c	Silt content /%	Clay content /%
42	1.94	2.70	1.08	46.2	26.4	10^{-8} – 10^{-6}	13.6	12.5	0.29	30.4	69.6

The content of clay particles (particle size smaller than 0.005 mm) accounts for 69.6% of the total amount, and the content of silt particles (0.005 mm < particle size < 0.075 mm) accounts for 30.4% of the total amount. According to the *Standard for geotechnical testing methods* (GB/T 50123-2019)^[14], the test soil sample is fine-grained soil. According to the classification standard of the plastic graphs of fine-grained soil, the soil sample is clay with low liquid limit (CL).

2.2 Test scheme

To analyze the engineering characteristics of soft clay under dynamic–seepage coupling conditions, a series of cyclic dynamic triaxial tests was conducted on the undisturbed soil under different seepage forces. During the test, while opening the lower pore pressure valve of the GDS dynamic triaxial instrument, a back pressure was applied to the top end of soil through the back pressure controller, thus leading to a water pressure difference between top and bottom of the sample, that is, the seepage force. Meanwhile, a set of undrained cyclic dynamic triaxial

tests without considering seepage was carried out to explore the effect of seepage on the dynamic characteristics of soft clay. Since the groundwater level of the sampling site is 2–4 m, and the general underground engineering activities are within a range of dozens meters depth, the design seepage force is in the range of 50–150 kPa, which is only used as preliminary investigation under the dynamic–seepage coupling conditions.

To ascertain the influence of the cyclic stress ratio and vibration frequency on the dynamic characteristics of soft clay in the dynamic–seepage coupling field, the cyclic stress ratios (CSR) are selected as 0.1, 0.2, 0.3 and 0.4, the vibration frequencies are 0.5, 1.0, 2.0, 3.0 and 4.0 Hz. The calculation formula of the cyclic stress ratio is as follows:

$$\text{CSR} = \frac{\sigma_d}{2\sigma_3} \quad (1)$$

where σ_d is the dynamic stress amplitude (kPa); σ_3 is the consolidation pressure (kPa). The vibration waveform

is a sine wave, and the test plan is shown in Table 2.

Table 2 Scheme of triaxial tests under confining pressure of 100 kPa

Seepage force /kPa	CSR	Frequency /Hz	Cycle number <i>N</i>
50	0.2	1.0	5 000
80	0.2	1.0	5 000
100	0.2	1.0	5 000
120	0.2	1.0	5 000
150	0.2	1.0	5 000
50	0.1	1.0	5 000
50	0.2	1.0	5 000
50	0.3	1.0	5 000
50	0.4	1.0	5 000
50	0.2	0.5	5 000
50	0.2	1.0	5 000
50	0.2	2.0	5 000
50	0.2	3.0	5 000
50	0.2	4.0	5 000
—	0.3	1.0	5 000
50	0.3	1.0	5 000

In particular, it is different from the typical drained triaxial test, the accumulated excess pore water pressure can be dissipated due to the intrinsic setting of drainage conditions during vibration loading in the drained (or partial drained) triaxial test. In this case, the dynamic pore pressure is generated "passively". In the test plan of this study, the water head is controlled artificially, which can be considered as a kind of "actively" generated volume force. The soil sample in this test has a high fines content and does not have liquefaction potential, so it will not be discussed.

2.3 Test procedures

(1) Sample preparation. The undisturbed soil taken out of the thin-walled soil extractor is cut on the soil cutter according to the *Standard for geotechnical testing methods* (GB/T 50123-2019)^[4] to make a sample with a diameter of 39.1 mm and a height of 80 mm.

(2) Saturation. (i) Saturation by vacuuming: Put the three-axis saturator with the sample into the vacuum cylinder and seal it, connect the vacuum cylinder to the aspirator to pump to the vacuum state, and maintain it for 12 hours. Gently open the liquid inlet pipe, and slowly pour clean water into the vacuum cylinder until the water floods the saturator and then stop pumping. Open the vacuum cylinder cover, and rest for more than 12 hours, so that the sample is fully saturated. (ii) Back pressure saturation: After installing the sample to the GDS triaxial instrument, use the back pressure setting to perform secondary saturation, and stop saturation when the *B* value reaches 0.95. The calculation formula of *B* value is as follows:

$$B = \frac{\Delta u}{\Delta \sigma_3} \quad (2)$$

where Δu is the increment of pore pressure (kPa); $\Delta \sigma_3$ is the increment of confining pressure (kPa).

(3) Anisotropic consolidation. Since the coefficient of earth pressure at rest K_0 for cohesive soil is usually between 0.5 and 0.8, the consolidation ratio in this study is a relatively conventional value of 1.5. When the pore water pressure dissipates to the back pressure or the axial strain rate becomes stable, the consolidation is considered complete.

(4) Dynamic loading. Open the drain valve as the seepage outlet, and set an upper back pressure as the seepage inlet to form a stable seepage field. The cyclic load waveform is selected as a sine wave, and the vibration frequency, cyclic stress amplitude and vibration times are set according to the test plan. During the loading process, the computer automatically collects and records test data such as loading time, axial stress, and strain.

(5) Unloading and uninstalling sample. Unload the load, remove the soil sample, and finally clean the instrument.

3 Experimental results and analysis

3.1 Strain development

3.1.1 Influence of seepage force

Figure 1 shows the cumulative plastic strain development curve of soft clay subjected to different seepage forces with the cyclic stress ratio $CSR = 0.1$ and the frequency $f = 1$ Hz. It is observed that the cumulative plastic strain presents a three-stage development law: in the initial stage of vibration, it increases approximately linearly to 30%–40% of the total strain; the cumulative plastic strain in the middle stage of the vibration shows a slow increase trend; next, the plastic strain develops into a stable or non-convergent development mode. For the convenience of analysis, this study defines the two types as follows:

$$\Delta \varepsilon_p \Big|_{\Delta N=1000} \leq 0.01\% \quad (3)$$

where $\Delta \varepsilon_p$ is the cumulative plastic strain increment; ΔN is the cyclic vibration increment.

That is, in the later stage of cyclic loading, when the number of cycle increases by 1 000 and the cumulative plastic strain increment is not more than 0.01%, the curve development form is stable; otherwise, it is development type.

The seepage force has a significant effect on the development of cumulative plastic strain. The greater the seepage force is, the greater the cumulative plastic strain is. The linear instantaneous growth rate of strain at the initial stage of vibration under different seepage forces is not much different. The main reason is that this stage is the shear deformation of saturated soft clay under instantaneous loading. The influence of seepage force is mainly reflected in the decelerating growth phrase

of strain in the middle stage of vibration loading. With the increase of the cyclic load period, the volume deformation of drained consolidation accounts for the main stage. Fig. 1 shows that when the number of cyclic vibrations exceeds 2 000, the plastic deformation of the soil under 50 kPa and 80 kPa seepage forces does not change extremely with the development of the number of cycle. When each vibration increases by 1 000, the cumulative plastic strain increment is smaller than 0.01%, its development mode is stable, and finally reaches a relatively stable state, while the deformation under other large seepage forces is finally developed, and the average cumulative plastic strain is 0.06% with the increase of 1 000 cycles. After the deceleration of growth phase is over, the deformation of the stable type is more than 90% for the total deformation, and the cumulative deformation of the development type is smaller than 85% for the total deformation. The greater the seepage force is, the greater the final cumulative plastic strain is. When the seepage force increases from 50 kPa to 150 kPa, the cumulative plastic strain increases by 1–2 times.

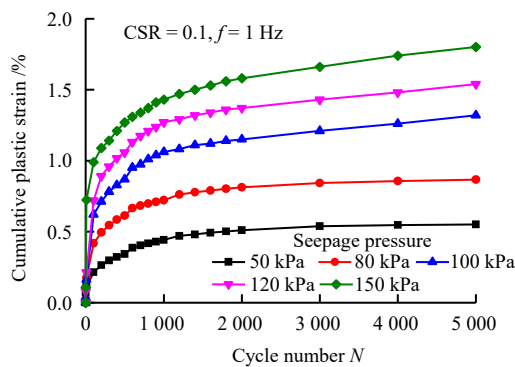


Fig. 1 Cumulative plastic strains under different seepage pressures

In the dynamic-seepage field, when the consolidated confining pressure is constant, the greater the seepage force, the more significant the plastic deformation of the soft clay. The seepage force causes the smaller soil particles to rotate, move and even break, showing compaction characteristics along the seepage direction. Meanwhile, under the action of the coupled cyclic load, the pore water in the soil mass is continuously discharged from the mass through seepage movement, the soil mass undergoes dynamic drainage and consolidation, pore compression, soil skeleton compaction, as a result, the soil mass exhibits a large deformation.

3.1.2 Influence of cyclic stress ratio

Figure 2 shows the cumulative plastic strain development of soft clay under different cyclic stress ratios when the frequency $f = 1$ Hz and the seepage force $p = 50$ kPa. It is observed that the influence of the cyclic stress ratio on cumulative plastic strain of soft clay is similar to that of seepage force, and its development curve

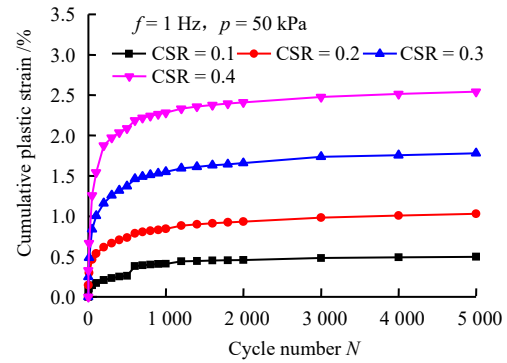


Fig. 2 Cumulative plastic strains under different cyclic stress ratio

shows a three-stage development law. When $CSR = 0.1$, at the end of the vibration period ($N: 4\ 000 \rightarrow 5\ 000$), $\Delta\varepsilon_p|_{\Delta N=1\ 000} = 0.005\ 9\%$, the soil deformation is stable type, and it enters a stable development stage at about 2 000 cycles, with a strain exceeding 90% of the total deformation. With the increase of dynamic stress, the plastic strain of soft clay gradually transforms from stable to developing. In the later stage of vibration, plastic strain still accumulates at a small rate, and the strain accumulation rate is not much different under different cyclic stress ratios. At the end of vibration, the cumulative plastic strain under the condition of cyclic stress ratio for 0.1 is 0.54%. When the cyclic stress ratio increases to 0.4, the cumulative plastic strain increases by 3.87 times.

Cyclic loading promotes soil dynamic drainage and consolidation, pore water is discharged from the soil mass, pore is compressed, and volumetric strain is generated. As such, the larger soil particles are broken into smaller particles under the action of cyclic loading, and the smaller particles are compressed and reorganized to form a denser soil skeleton, which causes greater deformation. The greater the cyclic stress ratio, the more significant the effect of dynamic drainage consolidation, the greater the degree of soil particle fragmentation, and the larger the plastic deformation.

3.1.3 Influence of frequency

Figure 3 displays the cumulative plastic strain development of soft clay under different vibration frequencies when the cyclic stress ratio $CSR = 0.2$, and the seepage force $p = 50$ kPa. It is shown that the vibration frequency has a significant effect on the cumulative plastic strain development of soft clay. The accumulative plastic strain growth rates at different frequencies in the initial period of vibration are basically same. In the middle period of vibration, the influence of frequency is more prominent. The smaller the frequency, the greater the plastic strain. When the frequency is 4 Hz, at the end of vibration ($N: 4\ 000 \rightarrow 5\ 000$), $\Delta\varepsilon_p|_{\Delta N=1\ 000} = 0.009\ 3\%$, the plastic deformation of soft clay develops into a stable type. When the cycles are higher than 2 000, the deformation is basically stable, and the deformation reaches 90% of the total

deformation. When the frequency is lower than 4.0 Hz, as the vibration frequency decreases, the development rate of soil deformation accelerates, resulting in greater plastic deformation. At the end of the vibration, the cumulative plastic strain at 0.5 Hz is 2.47 times that at 4.0 Hz.

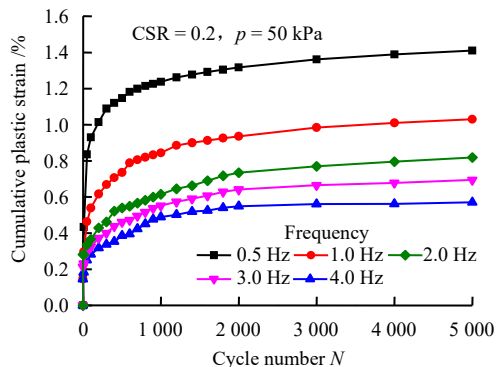


Fig. 3 Cumulative plastic strains under different frequencies

Aiming at the mechanism of frequency influence, Yang et al.^[15] considered that under low frequency conditions, the external load had stronger effect on the specimen, which results in a greater the damage to the structural connection between soil particles under all other conditions being the same, causing a greater the plastic deformation. Wang et al.^[16] explained the influence of frequency on dynamic deformation from the perspective of energy, and proposed the cumulative effect at low frequencies. They observed the frequency effect increased significantly as the frequency increased. Wang et al.^[17] noticed that the pore pressure had sufficient time to accumulate under low frequency conditions (<0.1 Hz), thereby affecting the deformation characteristics. This study believed from the perspective of energy analysis that, because the mechanical behavior of soft clay had certain visco-elastoplastic characteristics, under the same number of cycle. Because the higher the frequency, the higher the loading rate, and the shorter the overall time for the soft clay to absorb energy. As a result, the capability of energy absorption due particle rearrangement and pore compaction is relatively low, resulting in a smaller deformation.

3.1.4 Prediction model for accumulative plastic strain

Scholars have done a lot of work on the development and prediction model of cumulative plastic deformation of soft clay under cyclic loading. The parameters of theoretical analysis based on constitutive models are difficult to obtain, the calculation amount is large, and the calculation results often differ greatly from the actual project, consequently the applicability is not great. The empirical model is widely used because of its simplicity and convenience. The most widely used is the exponential model proposed by Monismith^[18]:

$$\varepsilon_p = aN^b \quad (4)$$

where ε_p is the cumulative plastic strain (%); a and b are the test parameters. Li et al.^[19] proposed a modified model that considers the dynamic stress level, the static strength of the soil and the physical and mechanical properties based on the exponential model:

$$\varepsilon_p = a \left(\frac{\sigma_d}{\sigma_s} \right)^m N^b \quad (5)$$

where σ_s is the static strength of the soil (kPa); m is the test parameter. After that, Chai et al.^[20] further modified the exponential model and added the initial deviatoric stress to obtain the following empirical model:

$$\varepsilon_p = a \left(\frac{\sigma_d}{\sigma_s} \right)^m \left(1 + \frac{\sigma_{id}}{\sigma_s} \right)^n N^b \quad (6)$$

where σ_{id} is the initial deviatoric stress; n is the test parameter. It can be found that, for the long-term deformation prediction model of soft clay under dynamic loading, its framework mainly contains three aspects: (i) the part of the function reflecting the initial state of the soil, such as the consideration of the initial static deviatoric stress by Chai et al.^[20], and the CSR consideration of the over-consolidation degree of the soil by the modified model of Chen et al.^[21]; (ii) functional parameters reflecting the loading conditions, such as dynamic stress amplitude, frequency and other parameters; and (iii) functional model that reflects periodicity. The mathematical relationship that characterizes the evolution mode of soil deformation, such as the exponential form or power function form of the vibration.

Based on the Monismith exponent model, this study considers the effects of seepage force, cyclic stress ratio and vibration frequency on the cumulative plastic deformation, and establishes a prediction model for the cumulative plastic deformation of soft clay in the dynamic-seepage field^[22]:

$$\varepsilon_p = ae^{\left(\frac{p}{\sigma_3} + \text{CSR} \right)} f^k N^b \quad (7)$$

where k is the test parameter; p is the seepage force (kPa); and f is the frequency. Through multiple regression mathematical analysis, Table 3 gives the fitting parameters and the coefficient of determination under different conditions. Statistics show that the range of parameter a is 0.029–0.058, b is 0.128–0.184, m is 2.982–6.452, and k is –0.567––0.704. The variance R^2 of the fitted curves are all above 0.85. Fig.4 shows the comparison between the prediction model and the test data under different conditions. It is observed that within a certain error tolerance range, the prediction model can well reflect the development law of cumulative plastic deformation of soft clay considering the effects of seepage.

Table 3 Parameters of the proposed model

Seepage force /kPa	CSR	Frequency /Hz	a	m	k	b	R^2
50	0.2	1.0	0.057 6	3.282 5	—	0.159 8	0.952 1
80	0.2	1.0	0.056 4	3.808 1	—	0.172 5	0.922 1
100	0.2	1.0	0.058 4	2.980 7	—	0.173 9	0.906 3
120	0.2	1.0	0.057 5	3.496 7	—	0.164 5	0.897 5
150	0.2	1.0	0.058 1	3.097 3	—	0.148 4	0.943 5
50	0.1	1.0	0.039 6	6.012 7	—	0.184 3	0.899 7
50	0.2	1.0	0.030 6	5.987 3	—	0.159 8	0.964 9
50	0.3	1.0	0.034 9	6.216 3	—	0.143 9	0.922 8
50	0.4	1.0	0.029 1	6.452 3	—	0.129 5	0.867 1
50	0.2	0.5	0.028 6	4.498 7	-0.638 7	0.128 1	0.896 2
50	0.2	1.0	0.029 4	4.789 2	—	0.159 8	0.964 9
50	0.2	2.0	0.031 2	5.013 4	-0.566 8	0.172 9	0.975 3
50	0.2	3.0	0.030 1	5.285 1	-0.703 5	0.168 5	0.973 8
50	0.2	4.0	0.291 6	4.872 9	-0.673 5	0.163 0	0.951 0

3.2 Dynamic parameters

3.2.1 Hysteretic curve

Figure 5 shows the hysteretic curve of soft clay at different loading stages for $CSR = 0.3$ and $f = 1$ Hz. It is found that the hysteretic curve has obvious characteristics of non-linearity and hysteresis. Its shape is similar to an ellipse and is not closed, which characterizes the residual strain under each cycle. As the number of cycles increases, the residual strain gradually decreases or even disappears, indicating that the cumulative plastic strain of soft clay will eventually converge to a stable value. The hysteretic curve gradually inclines slightly to the strain axis, and the shape gradually transitions from the "date pit-shaped" full state to the "needle-shaped" lean state, which indicates that the energy dissipation of the soil has decreased, and the soil will mainly show elastic behavior.

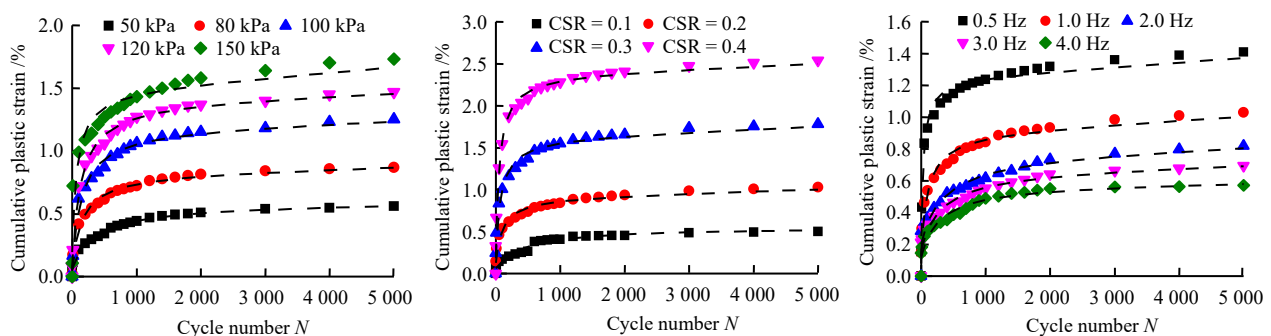
The existence of seepage force has an effect on the hysteretic curve of soft clay. In the initial stage of vibration, under the condition of seepage force, the hysteretic curve of soft clay is inclined to the strain axis more than that under the condition of no seepage, which indicates that its dynamic modulus is smaller, and its shape is less full. The stress amplitude and strain amplitude are generally smaller than those under non-seepage conditions. When the number of cycles surpasses 100, there is little difference in the shape of the hysteretic curve under the conditions of seepage and non-seepage, and the shape

of the hysteresis curve is approximately coincident. This shows that the effect of seepage force on the dynamic stress–strain relationship is mainly reflected in the initial stage of vibration. The reason for this phenomenon is that in the initial stage of dynamic loading, due to the extra presence of seepage force, the pore water has no time to drain. Under the same axial stress value, the dynamic strain response generated is greater than that without seepage force. As a result, the degree of inclination of the hysteretic curve to the strain axis increases, and with the continuous increase of the number of vibrations, due to the influence of dynamic drainage and consolidation, pore water is discharged, the influence of seepage force on the hysteretic curve is weakened. Therefore, the hysteretic loop shape gradually approaches that without seepage.

3.2.2 Dynamic modulus

(1) Influence of seepage force

Figure 6 shows the development curves of soft clay dynamic elastic modulus with number of cycles under different seepage forces for $CSR = 0.2$ and $f = 1$ Hz. In general, the dynamic model shows a development law of short-term increase and slow decrease in the later period, and the greater the seepage force is, the smaller the dynamic elastic modulus is. Under low seepage force (50–80 kPa), the dynamic elastic modulus attenuates after 1 000 vibrations, and under higher seepage force (greater than 100 kPa), the dynamic modulus begins to

**Fig. 4** Performance of the proposed model under different conditions

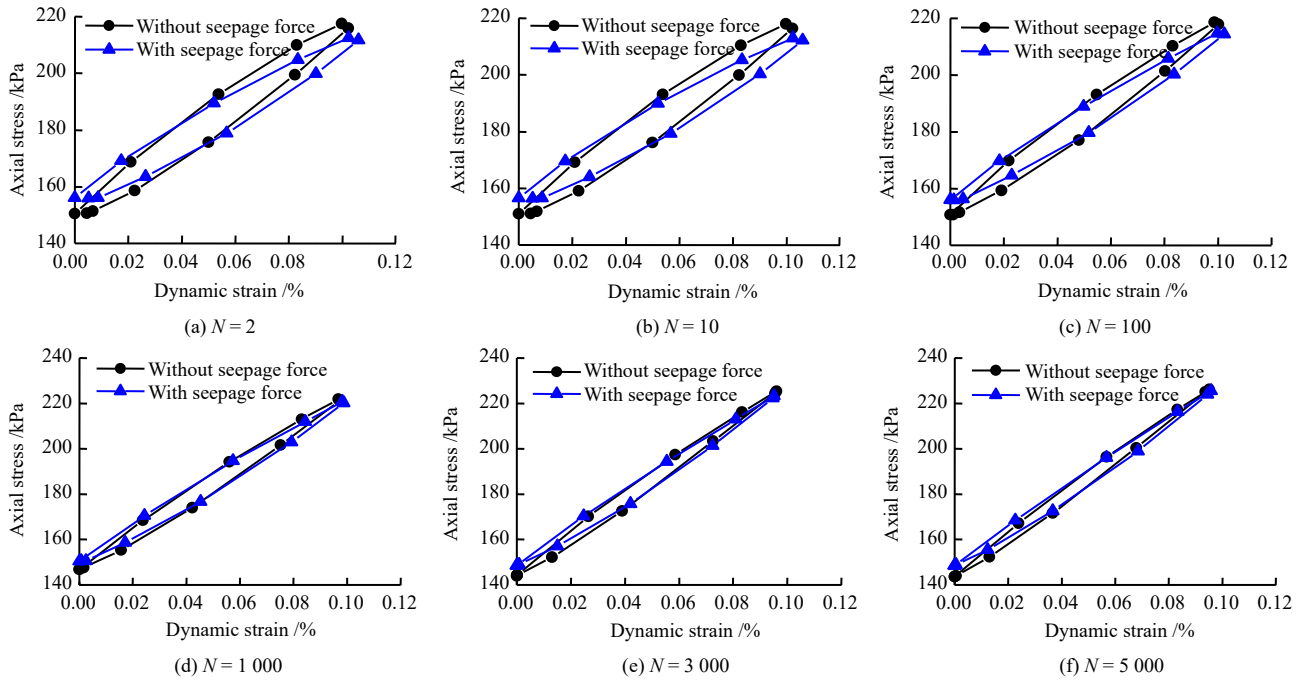


Fig. 5 Hysteretic curves of soft clay under different number of cycles

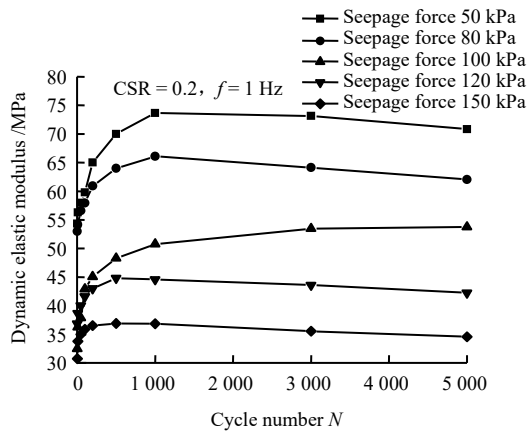


Fig. 6 Dynamic elastic modulus under different seepage

degrade after 500 vibrations, with reduction of 5.7% and 6.3%, respectively. This indicates that with the increase of seepage force, the time for the dynamic elastic modulus to reach the peak is shorting. After 5 000 vibrations, the dynamic elastic modulus under 150 kPa seepage force is 34.6 MPa, which is an increase of 12.4% from the initial value; and the dynamic elastic modulus under 50 kPa seepage force is 70.8 MPa, which is an increase of 30.3% relevant to the initial value.

Considering the influence of seepage force, at the initial stage of vibration, due to the instantaneous loading of soil, the pore water is too late to discharge and there is no volume deformation, resulting in the initial increase of dynamic elastic modulus. With the increase of number of cycles, the pore water is discharged out of the soil mass under the coupling effect of dynamic-seepage, the pore volume is reduced, the soil skeleton is compacted, and the soil is dynamically drained and consolidated. With the development of volume deformation, the dynamic elastic modulus shows a decreasing law. In the later stage

of vibration, with the compaction of the soil skeleton stabilizes, the dynamic elastic modulus tends to stabilize, and the deformation gradually stabilizes, too.

(2) The relationship between dynamic elastic modulus and cumulative plastic strain

For the convenience of analysis, δ is defined as the conversion coefficient of dynamic elastic modulus:

$$\delta = \frac{1}{E_d} \quad (8)$$

where E_d is the dynamic elastic modulus (MPa).

Figure 7 shows the change of the conversion coefficient of dynamic elastic modulus with cumulative plastic strain under different cyclic stress ratios with frequency $f = 1$ Hz, seepage force $p = 50$ kPa. It is indicated that with the development of cumulative plastic strain, the conversion coefficient δ approximately attenuates in a power function. Under the different CSRs, the difference of δ is not obvious, which shows that the CSR has no significant influence on δ , and the change of δ mainly depends on the development of plastic strain.

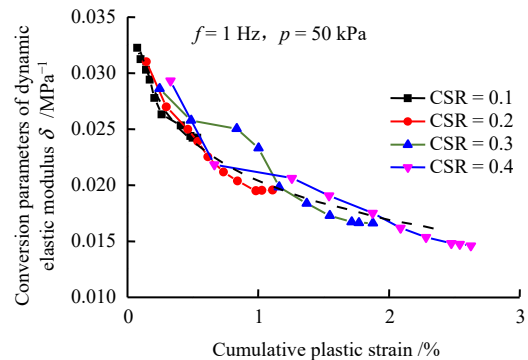


Fig. 7 Dynamic modulus versus cumulative plastic strain under different cyclic stress ratio

Figure 8 presents the development of dynamic elastic modulus with cumulative plastic strain at different frequencies. It is indicated that with the number of vibrations increases, the conversion coefficient δ generally displays a quadratic function change law, and with decreasing frequency, its strain amplitude and critical strain value at the inflection point gradually increase. This phenomenon is mainly related to the development mode of cumulative plastic strain. According to Fig. 3, when the frequency is high, the cumulative plastic strain tends to be stable, and the dynamic elastic modulus gradually rises to a stable value with the increase of soil compaction; when the frequency is low, the cumulative plastic strain continues to increase, the shear deformation continues to increase, and the dynamic elastic modulus gradually decreases. Since the conversion coefficient and the dynamic elastic modulus are reciprocal to each other, a quadratic function distribution appears.

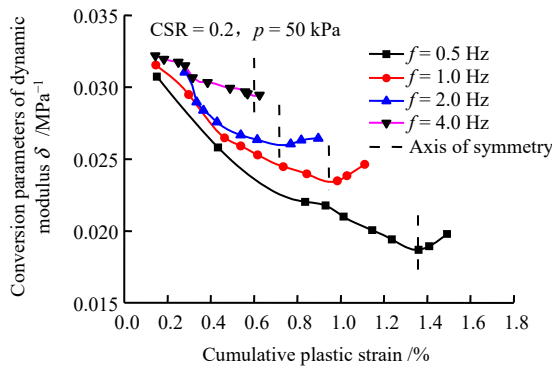


Fig. 8 Dynamic elastic modulus versus cumulative plastic strain under different frequencies

Figure 9 is the δ - ε_p curves of soft clay δ - ε_p under different seepage forces. It is shown that the seepage force has a greater influence on δ . As the seepage force rises, δ gradually increases. It is shown that δ - ε_p approximately presents a quadratic function distribution, and the symmetrical axis strain is about 1%, which shows that the seepage force has little effect on the quadratic function morphology distribution, and the main influence is the extremum. The reason for the quadratic function distribution is similar to the influence mechanism at different frequencies.

Figures 8 and 9 illustrate that frequency and seepage force are closely related and have a significant impact on δ . For the convenience of analysis, the seepage force $p^{0.7}$ is used to normalize δ , and the normalized distribution of δ approximates to a quadratic function distribution. Meanwhile, the analysis combined with of Figs. 8 and 9 indicates that the variation of frequency affects the position distribution of the quadratic function, and the seepage force mainly affects the peak point of the function. Starting from the correlation between the two, considering the influence modes and mechanisms of seepage force and frequency, a normalized prediction

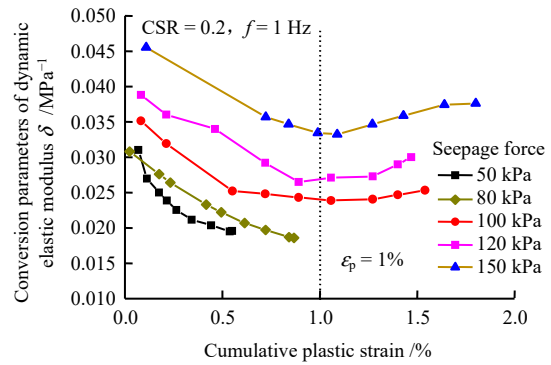


Fig. 9 Dynamic modulus versus cumulative plastic strain under different seepage forces

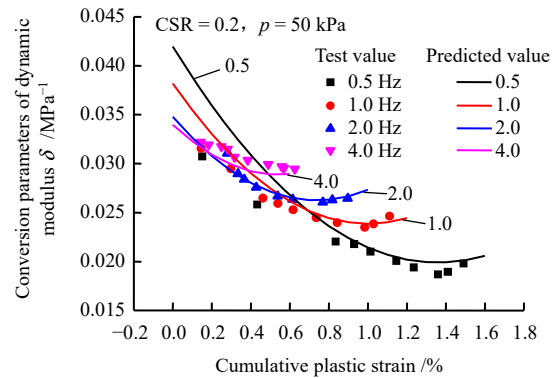


Fig. 10 Performance of the prediction model of dynamic elastic modulus under different frequencies

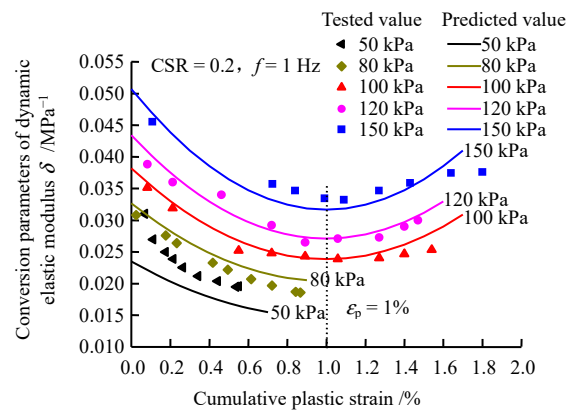


Fig. 11 Performance of the prediction model of dynamic elastic modulus under different seepage force

model is established as follows:

$$\frac{\delta}{f^* p^{0.7}} \times 10^4 = 5.7 \times \left(\varepsilon_p - \frac{1}{f^{0.44}} \right)^2 + 9.5 \quad (9)$$

where f^* is the frequency influence factor, $f^* = 1.1^{\log_2 f}$.

Figure 10 shows the comparison between the dynamic elastic modulus prediction curve and the test points under different frequency conditions. It is shown that the prediction model can well predict the dynamic elastic modulus of soft clay under different vibration frequencies.

Figure 11 is the comparison between the prediction curves of the soft clay dynamic elastic modulus under different seepage forces and the test points. It is shown that when the seepage force is large, exceeding 100 kPa,

the model prediction is better, and the seepage force is lower (<80 kPa), there is a certain deviation between the predicted value and the measured value, which is caused by the error of normalization. In general, the prediction is reasonably well, and the dynamic elastic modulus of soft clay can be estimated under the coupled condition of dynamic-seepage. The predicted model is suitable for the analysis of the dynamic characteristics for the site under the cyclic stress ratio lower than 0.4 and the frequency is smaller than 4 Hz.

3.2.3 Damping ratio

Damping ratio, as an important parameter of soil dynamics, reflects the hysteresis of the soil stress–strain relationship^[23]. The general calculation method is

$$\lambda = \frac{1}{4\pi} \frac{S_c}{S_{\Delta OAB}} \quad (10)$$

where λ is the damping ratio; S_c is the area of the hysteresis loop; and $S_{\Delta OAB}$ is the area of the triangle OAB , as shown in Fig. 12.

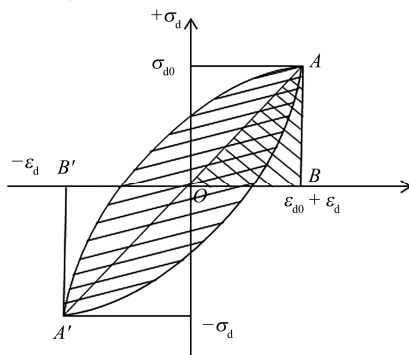


Fig. 12 Diagram of hysteretic curves

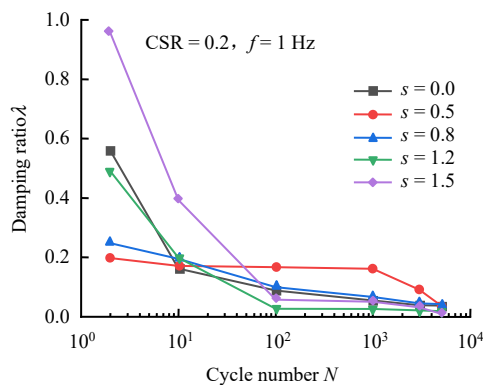


Fig. 13 Damping ratio curves with number of cycles

Figure 13 displays the variation curves of damping ratio with number of cycles subjected to different seepage forces under the conditions of $CSR = 0.2$ and $f = 1$ Hz. It is indicated that the damping ratio gradually attenuates to a stable value with the number of cycles. The existence of seepage force has a great influence on the damping ratio. For the convenience of analysis, the seepage ratio s is defined as

$$s = \frac{p}{\sigma_c} \quad (11)$$

where σ_c is the confining pressure (kPa).

At the initial stage of vibration, the damping ratio is 0.56 under no seepage conditions, and 0.16 after 10 cycles, which quickly attenuates by 71%. With the number of cycles continues to increase, the attenuation rate decreases. When the number of cycles reaches 5 000, the damping ratio attenuates to an approximate constant value of 0.04. When the seepage ratios are 1.2 and 1.5, the damping ratios are attenuated by 96% and 98%, respectively; and when the seepage ratios are 0.5 and 0.8, the damping ratios are attenuated by 79% and 83%, respectively. This suggests that as the seepage force increases, the attenuation amplitude of the damping ratio gradually increases. When the seepage ratios are 0.5 and 0.8, the change range of the damping ratio is relatively small. Compared with the non-seepage condition, the initial damping ratio (within 10 cycles) under seepage is only about 1/3 that in the no seepage condition. When the number of cycle exceeds 10, the damping ratio change is approximate to that under no seepage condition.

When the seepage ratios are 1.2 and 1.5, the effect of seepage force on the damping ratio is more significant. The initial damping ratio (within 10 vibrations) increases with the increase of seepage force. When the seepage ratio is 1.5, the initial damping ratio is 1.7 times that under no seepage condition. As the number of cycles increases, there is a sharp attenuation in the initial stage of loading, and then the attenuation rate slows. As the seepage ratio increases from 1.2 to 1.5, the stable value of the damping ratio declines from 0.02 to 0.01.

The analysis indicates that the change of the damping ratio for the soft clay under the coupled condition of dynamic-seepage is related to the seepage ratio. In general, the greater the seepage ratio is, the greater the attenuation amplitude of the damping ratio is. However, at the end of the vibration, the damping ratios of the samples under different seepage ratios are relatively close, approximately 0.02–0.04.

4 Conclusions

In this study, a series of dynamic-seepage coupled cyclic triaxial tests was carried out on saturated soft clay, and the cumulative plastic strain development laws of soft clay under different seepage forces, cyclic stress ratios and frequencies were analyzed, and a cumulative plastic strain prediction model was established; the changes of hysteresis curve, dynamic elastic modulus and damping ratio of soft clay were revealed, and the normalized mathematical model for dynamic elastic modulus and cumulative plastic strain was established. The main conclusions are as follows:

(1) The seepage force has an important influence on the cumulative plastic strain of soft clay. The seepage force increases the cumulative plastic deformation of

dynamic-seepage coupling by 1–2 times. The greater the seepage force, the greater the cumulative plastic strain, and its strain development presents three-stage characteristics: an initial instant increase, a moderate increase, and a stable/linear development. A greater dynamic stress with lower frequency results in a greater the cumulative plastic strain of soft clay. A predictive model of the cumulative plastic strain of soft clay considering the three factors of seepage force, frequency and cyclic stress ratio is established.

(2) The existence of seepage force increases the inclination of the hysteresis curve for soft clay to the strain axis; the dynamic elastic modulus of soft clay shows the characteristic of first increasing and then decreasing. The greater the seepage force, the lower the dynamic elastic modulus, and the smaller the critical number of cycles during attenuation. A normalized dynamic elastic modulus prediction model considering the seepage force and frequency is established.

(3) Under dynamic-seepage coupling conditions, the change of damping ratio is affected by seepage force. The greater the seepage force, the greater the attenuation amplitude of the damping ratio. The damping ratios under different seepage ratios are relatively close, approximately 0.02–0.04. The research results can provide a theoretical reference for site dynamic response analysis under fluid–structure coupling conditions.

References

- [1] ZHENG Gang, ZHAO Yue-bin, CHENG Xue-song, et al. Strategy and analysis of the settlement and deformation caused by dewatering under complicated geological condition[J]. China Civil Engineering Journal, 2019, 52(Suppl.1): 135–142.
- [2] LEI H Y, XU Y G, JIANG M J, et al. Deformation and fabric of soft marine clay at various cyclic load stages[J]. Ocean Engineering, 2019, 195: 106757.
- [3] LEI Hua-yang, JIANG Yan, LU Pei-yi, et al. Experimental study of dynamic constitutive relation of structural soft soils under traffic loading[J]. Rock and Soil Mechanics, 2009, 30(12): 3788–3792.
- [4] ZHENG Gang, HUO Hai-feng, LEI Hua-yang, et al. Contrastive study on the dynamic characteristics of saturated clay in different vibration frequencies[J]. Journal of Tianjin University (Science and Technology), 2013, 46(1): 38–43.
- [5] DING Zhi, ZHANG Tao, WEI Xin-jiang, et al. Experimental study on effect of different drainage conditions on dynamic characteristics of soft clay under different degrees of consolidation[J]. Chinese Journal of Geotechnical Engineering, 2015, 37(5): 893–899.
- [6] WEI Xin-jiang, ZHANG Tao, DING Zhi, et al. Experimental study on stiffness change of saturated soft clay with different degrees of consolidation under cyclic loading[J]. Chinese Journal of Geotechnical Engineering, 2013, 35(Suppl.2): 675–679.
- [7] LIU Jia-shun, WANG Lai-gui, ZHANG Xiang-dong, et al. Cyclic triaxial test on saturated silty clay under partial drainage condition with variable confining pressure[J]. Rock and Soil Mechanics, 2019, 40(4): 1413–1419, 1432.
- [8] WANG Yu-ke, WAN Yong-shuai, FANG Hong-yuan, et al. Experimental study of cyclic behavior of soft clay under circle stress paths[J]. Rock and Soil Mechanics, 2020, 41(5): 1643–1652.
- [9] TANG Y Q, SUN K, ZHENG X Z, et al. The deformation characteristics of saturated mucky clay under subway vehicle loads in Guangzhou[J]. Environmental Earth Sciences, 2016, 75(5): 1–10.
- [10] LEI H Y, LI B, LU H B, et al. Dynamic deformation behavior and cyclic degradation of ultrasoft soil under cyclic loading[J]. Journal of Materials in Civil Engineering, 2016, 28(11): 04016135.
- [11] YE Zheng-qiang, LI Ai-qun, YANG Guo-hua, et al. Study of permeability for cohesive soil[J]. Journal of Southeast University, 1999, 29(5): 121–125.
- [12] GU Zhong-hua, GAO Guang-yun, WANG Jie-hu. Experimental study on effects of structural properties to permeability coefficient of soft clay in Shanghai[J]. Exploration Engineering (Drilling & Tunneling), 2004, 31(5): 1–3.
- [13] XU Jia-hai. Permeability of clay soil[J]. Journal of Hydraulic Engineering, 1962(5): 46–49.
- [14] Ministry of water resources of the people's republic of China. GBT 50123–2019 Standard for geotechnical testing method[S]. Beijing: China Planning Press, 2019.
- [15] YANG Ai-wu, KONG Ling-wei, GUO Fei. Accumulative plastic strain characteristics and growth model of Tianjin Binhai soft clay under cyclic loading[J]. Rock and Soil Mechanics, 2017, 38(4): 979–984.
- [16] WANG Xin, SHEN Yang, WANG Bao-guang, et al. Failure criteria for soft clay subjected to frequencies under train loads[J]. Chinese Journal of Geotechnical Engineering, 2017, 39(Suppl.1): 32–37.
- [17] WANG Jun, CAI Yuan-qiang, XU Chang-jie, et al. Study on accumulative plastic strain model of soft clay under cyclic loading[J]. Chinese Journal of Rock Mechanics and Engineering, 2007(8): 1713–1719.
- [18] MONISMITH C L, OGAW N, FREEME C R. Permanent deformation characteristics of subgrade soils due to repeated loading[J]. Transportation Research Record, 1975, 537: 1–17.
- [19] LI D, SELIG E T. Cumulative plastic deformation for fine-grained subgrade soils[J]. Geotechnical Engineering, 1996, 122(12): 1006–1013.
- [20] CHAI J C, MIURA N. Traffic-load-induced permanent deformation of road on soft subsoil[J]. Journal of Geotechnical and Geoenvironmental Engineering, 2002, 128(11): 907–916.
- [21] CHEN Ying-ping, HUANG Bo, CHEN Yun-min. Reliability analysis of high level backfill based on chaotic optimization[J]. Chinese Journal of Geotechnical Engineering, 2008, 30(5): 764–768.
- [22] MIAO Jiang-yan. Experimental study on dynamic characteristics of soft clay considering seepage effect[D]. Tianjin: Tianjin University, 2018.
- [23] CHEN Wei, KONG Ling-wei, ZHU Jian-qun. A simple method to approximately determine the damping ratio of soils[J]. Rock and Soil Mechanics, 2007, 28(Suppl.1): 789–791.